CONF-770807--11

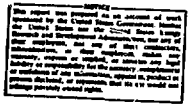

CREEP BUCKLING ANALYSIS OF SHELLS*

C. M. Stone

R. E. Nickell

Design Technology Division
Sandia Laboratories, Albuquerque, NM 87115

*This work supported by the United States Nuclear Regulatory Commission under ERDA Contract AT(29-1)-789.

I. Introduction

Thin-walled structural members that are subjected to sustained loads while at elevated temperature may exhibit a time-dependent structural instability, referred to as creep buckling. This term is meant to describe the process by which time-dependent inelastic behavior of the material interacts with initial imperfections and/or instantaneous, load-induced displacements so that amplification of these imperfection/displacements creates an unstable geometric configuration with respect to the applied loading.

Because of the characteristics of LMFBR primary piping components (thin-walled, low pressure, high temperature), the designer must guard against creep buckling as a potential failure mode for certain critical regions, such as elbows, where structural flexibility and inelastic respons may combine to concentrate deformation and cause instability. The ASME Boiler and Pressure Vessel Code, through its elevated temperature Code Case 1592 (Section III, Division 1) provides design rules for Class 1 components aimed at preventing creep buckling during the design life. A similar set of rules is being developed for Class 2 and Class 3 components at this time

One of the original concepts behind the creep buckling rules was that the variability in creep properties (especially due to the effects of prior heat treatment), the uncertainty about initial imperfections, and the lack of confirmed accuracy of design analysis meant that conservatism would be difficult to assure. As a result, a factor of ten on service life was required (i.e., analysis must show that, under service conditions that extrapolate the life of the component by ten times, creep buckling does not occur). Two obvious problems with this approach are that: first, the creep behavior must also be extrapolated (since most creep experiments are terminated at a small fraction of the design life, extrapolation of creep data is already an issue, irrespective of the creep buckling question); second, the nonlinear creep analysis, which is very nearly prohibitively expensive for design life histograms, becomes even more costly.

Primarily due to these two issues the creep buckling design rules were altered in order to accommodate load and strain factors of safety that were thought to be roughly equivalent to the factor of ten on service life. The background for the selection of these safety factors is given in a recent paper by Berman, et al. [1]*. In this report the specific concern is for the case of load-controlled time-dependent buckling, where the load factor is 1.5 for normal, upset, and emergency operating conditions, and 1.25 for faulted operating conditions. The motivation for the current study is to determine whether the materials behavior is consistent with adoption of these rules.

In order to test the hypothesis that these load factors were roughly equivalent to a factor of ten on life, a simple geometry was needed to keep

*Numbers in brackets indicate references that are listed at the end of the text.

the analysis expense reasonable. Also, a geometry (with boundary conditions, loads, and good creep characterization) that had been experimentally taken through a range of buckling parameters was desirable. For these two reasons the aluminum cylinder work of Samuelson [2] was selected as the basis for this study. The study itself was divided into three parts: (1) a software verification part that was designed to show that an existing general purpose, nonlinear, finite element program was capable of successfully analyzing the problem; (2) a convergence part that examined different elements, meshes, and nonlinear computing strategies so that a near-minimum critical buckling time could be assured; and (3) the safety factor evaluation parameter calculations themselves.

In the following sections, these items are discussed in some detail. Section 2 describes the experiments conducted by Samuelson. Section 3 outlines the computational procedure by which the critical buckling times are calculated. Section 4 gives the essential results of this study, followed by a section that provides the conclusions and recommendations.

2. Experimental Basis

A simple problem geometry with supporting experimental work and with good material characterization was needed for this study. The experimental work done by Samuelson [2] on axially loaded aluminum cylinders provided the needed test results with which to evaluate the numerical calculations. In his work, Samuelson tested a series of 41 aluminum cylinders with various magnitudes of axial load and with ratios of cylinder radius to wall thickness (R/h) varying from 30 to 150. The length to radius ratio (L/R) in all cases was greater than 2. The tests were run at elevated temperature (225°C), with the material properties determined from special compressive creep specimens also tested at high temperature. From the creep data obtained during these special tests, Samuelson determined that the creep rate, $\dot{\bar{\varepsilon}}_c$, could be approximated by a power law on stress, σ.

$$\dot{\bar{\varepsilon}}_c = B\sigma^n \quad , \tag{1}$$

where the constants B and n were determined from the test data.

The cylinders were tested in a specially prepared loading frame with the shell edges inserted into machined slots in the loading device. It is important to note that radial growth resulting from a uniform thermal expansion of the cylinder will be restricted at the shell edges causing local bending near the supports. Application of the test load was done slowly to avoid introducing inertia effects; consequently, the critical time reported by Samuelson was the time elapsed from final application of the test load until the time of specimen collapse. The observed collapse mechanism was the rapid growth of bulges which appeared near the shell supports.

The dominant factor used in selecting a particular cylinder geometry

Samuelson's paper, the buckled configuration was characterized by the number of circumferential waves observed at collapse. It was felt that by choosing a test where the number of circumferential waves was zero, a computationally simple two-dimensional axisymmetric analysis could be performed. Seven cases of zero circumferential waves were observed in the 41 tests performed. The final selection was based on the shortest critical time measured for the seven cylinders. The test selected had the following characteristics: $R/h = 32$, $h = 1.495$ mm, $\sigma_{APPLIED} = 12.1$ kg/mm^2. The experimental results for this test show a critical time of 435 minutes (7.25 hours).

3. Numerical Procedure

Two numerical procedures come to mind for the solution of the time-dependent buckling problem. The first method, recently discussed by Miyazaki, et al. [3], entails time marching for a period of interest and evaluating the structure stiffness matrix at each time step. As the critical time is reached, the stiffness matrix becomes nonpositive definite, which corresponds to an instability of the physical structure. The main flaw with this method is that for most problems of interest (e.g., nuclear piping components) the time to collapse is quite long so that the computational expense is prohibitive. The second method allows a direct calculation of the critical time after only a few time steps. This direct procedure is quite attractive from a computational point of view and was chosen for the current numerical study. The computational details can be found in [4,5], but will be repeated here for completeness.

Let us define the linear elastic stiffness matrix as $\underset{\sim}{K}^{(0)}$, the initial stress matrix as $\underset{\sim}{K}^{(1)}(\underset{\sim}{\sigma})$, and the initial displacement matrix as $\underset{\sim}{K}^{(2)}(\underset{\sim}{u})$, where $\underset{\sim}{\sigma}$ and $\underset{\sim}{u}$ are the stress and displacement fields, respectively. The incremental equation of equilibrium is then

$$(\underset{\sim}{K}^{(0)} + \underset{\sim}{K}^{(1)}(\underset{\sim}{\sigma}) + \underset{\sim}{K}^{(2)}(\underset{\sim}{u})) \cdot \Delta\underset{\sim}{u} = \Delta\underset{\sim}{P} \qquad (2)$$

where the incremental load vector, $\Delta\underset{\sim}{P}$, is understood to include the effect of initial strains due to creep deformation for time-dependent buckling. For time-independent, load controlled buckling, $\Delta\underset{\sim}{P}$ would contain only incremental external loads, for time-dependent, strain controlled buckling, $\Delta\underset{\sim}{P}$ contains initial strains due to thermal loading.

As the nonlinear solution progresses, the analyst may wish to determine the load or time multiplier, λ, such that the forcing function, $\lambda\Delta P$, will cause the structural stiffness to become nonpositive definite. This nonlinear structural stiffness can be written

$$(\underset{\sim}{K}^{(0)} + \underset{\sim}{K}^{(1)}(\underset{\sim}{\sigma} + \lambda\Delta\underset{\sim}{\sigma}) + \underset{\sim}{K}^{(2)}(\underset{\sim}{u} + \lambda\Delta\underset{\sim}{u})) \quad , \qquad (3)$$

and if the stiffness is expanded about the state $(\underset{\sim}{\sigma},\underset{\sim}{u})$, the eigenvalue problem becomes

$$\underset{\sim}{K}^{(0)} + \underset{\sim}{K}^{(1)}(\underset{\sim}{\sigma}) + \underset{\sim}{K}^{(2)}(\underset{\sim}{u}) + \lambda(\Delta\underset{\sim}{K}^{(1)}(\Delta\underset{\sim}{\sigma}) + \Delta\underset{\sim}{K}^{(2)}(\underset{\sim}{u},\Delta\underset{\sim}{u}))$$

$$\underset{\sim}{\phi} = 0 \qquad (4)$$

where $\underset{\sim}{\phi}$ is the buckling mode shape corresponding to λ.

In (4) the calculation of $\underset{\sim}{K}^{(0)}$, $\underset{\sim}{K}^{(1)}$, and $\underset{\sim}{K}^{(2)}$ remain straight forward, but some comment on the numerical calculation of $\Delta\underset{\sim}{K}^{(1)}(\Delta\underset{\sim}{\sigma})$ and $\Delta\underset{\sim}{K}^{(2)}(\underset{\sim}{u},\Delta\underset{\sim}{u})$ is needed. The formation of $\Delta\underset{\sim}{K}^{(1)}(\Delta\underset{\sim}{\sigma})$ can be made quite simply when one recalls that $\underset{\sim}{K}^{(1)}$ is a linear function of $\underset{\sim}{\sigma}$ so that

$$\underset{\sim}{K}^{(1)}(\Delta\underset{\sim}{\sigma}) = \Delta\underset{\sim}{K}^{(1)}(\Delta\underset{\sim}{\sigma}) \quad . \qquad (5)$$

The calculation of $\Delta\underset{\sim}{K}^{(2)}(\underset{\sim}{u},\Delta\underset{\sim}{u})$ requires some additional work due to the higher order dependence of $\underset{\sim}{K}^{(2)}$ on the displacements, $\underset{\sim}{u}$. In order to determine $\Delta\underset{\sim}{K}^{(2)}$, we note that

$$\underset{\sim}{K}^{(2)}(\underset{\sim}{u}) = \underset{\sim}{B}^{(\ell)^T} \cdot \underset{\sim}{D} \cdot \underset{\sim}{B}^{(0)} + \underset{\sim}{B}^{(0)^T} \cdot \underset{\sim}{D} \cdot \underset{\sim}{B}^{(\ell)} + \underset{\sim}{B}^{(\ell)^T} \cdot \underset{\sim}{D} \cdot \underset{\sim}{B}^{(\ell)} \qquad (6)$$

where $\underset{\sim}{B}^{(0)}$ are the linear terms in the strain-displacement relations and $\underset{\sim}{B}^{(\ell)}$ are the corresponding nonlinear terms. The matrix $\underset{\sim}{B}^{(0)}$ is not a function of the displacements while the matrix $\underset{\sim}{B}^{(\ell)}$ is a linear function of $\underset{\sim}{u}$. The matrix $\underset{\sim}{D}$ is the elastic or elastic-plastic constitutive matrix. Expansion of $\underset{\sim}{K}^{(2)}(\underset{\sim}{u})$ in a Taylor series about the displacements, $\underset{\sim}{u}$, gives a final matrix form for $\Delta\underset{\sim}{K}^{(2)}$,

$$\Delta\underset{\sim}{K}^{(2)}(\underset{\sim}{u},\Delta\underset{\sim}{u}) = \underset{\sim}{B}^{(0)^T} \cdot \underset{\sim}{D} \cdot \overline{\underset{\sim}{B}}^{(\ell)} + \overline{\underset{\sim}{B}}^{(\ell)^T} \cdot \underset{\sim}{D} \cdot \underset{\sim}{B}^{(0)} + \overline{\underset{\sim}{B}}^{(\ell)^T} \cdot \underset{\sim}{D} \cdot \underset{\sim}{B}^{(\ell)} + \underset{\sim}{B}^{(\ell)^T} \cdot \underset{\sim}{D} \cdot \overline{\underset{\sim}{B}}^{(\ell)} \qquad (7)$$

where

$$\overline{\underset{\sim}{B}}^{(\ell)} = \underset{\sim}{B}^{(\ell)}(\Delta\underset{\sim}{u}) \quad .$$

The computational procedure used to determine the critical load involves use of incremental loading to reach a desired load level, P. The load is incremented by a value ΔP and the resulting matrix equations solved for the displacements. Using the displacements and corresponding stresses, the appropriate stiffness matrices are formed and the eigenvalue problem solved for λ and the bucking mode shape, $\underset{\sim}{\phi}$. The critical buckling load is then determined by

The time-dependent buckling problem is handled in a similar fashion. The load consists of initial-strain terms that are proportional to the time step, Δt (the initial-strain is proportional to $\dot{\bar{\varepsilon}}_c$ which, in incremental form, becomes $\Delta\bar{\varepsilon}_c = F(\sigma,t,\bar{\varepsilon}_c) \cdot \Delta t$). Therefore, in (8), the load P can be replaced with the time t and the incremental load ΔP with the time increment Δt. The resulting equation for the critical buckling time becomes

$$t_{CR} = t + \lambda\Delta t \quad . \tag{9}$$

The step-by-step procedure used for time-dependent buckling is as follows:

1. Apply external loads and solve the time-independent problem (elastostatic problem);
2. Begin to march in time for creep analysis;
3. Stop the creep analysis at a convenient time, t;
4. Allow a small additional creep increment, Δt;
5. Solve the resulting eigenvalue problem for λ and $\underset{\sim}{\phi}$;
6. Calculate the critical time using (9).

It is possible to obtain an even better estimate of the critical time by evaluating (9) at various times and extrapolating these results. An example of this procedure is given in the next section.

Although the procedure is simple, automatic application to every time-dependent buckling problem can lead to questionable results. For example, care must be taken, when using this method in conjunction with a residual load correction technique, to ensure that the incremental solution has converged. If the solution has drifted, large corrective forces may be added to the force vector. If a small creep increment, Δt, is used the resulting initial strain terms can be insignificant compared to the magnitude of the corrective forces. The resulting force vector is then no longer proportional to the time increment and any critical time estimate predicted would be incorrect.

A similar problem exists when the analysis indicates plasticity occurring simultaneously with creep. As long as the creep strains are large in comparison with the plastic strains, the numerical procedure can be used with some confidence. As the plastic strains become large, the structural stiffness reflects changes due to plasticity, as well as creep, and these changes are no longer proportional to the time increment; again, eq. (9) is no longer valid.

4. Numerical Results

The aluminum cylinder described in Section 2 was modeled as a two-dimensional axisymmetric body. The kinematic boundary conditions imposed on the model are shown in Fig. 1. The radial boundary condition applied at the top of the shell provides a model of the restraining action of the

L/R greater than 2.

The initial discretization used axisymmetric continuum elements with bilinear displacement approximations. Three elements were used in the radial direction and twenty elements were equally spaced along the length (see Fig. 2a). The test load of 12.1 kg/mm^2 was applied and the instantaneous elastic buckling load (Euler load) was calculated to be within ten percent of the classical value. The shell was then creep analyzed to a time of one hour. The estimated time of collapse for the perfect cylinder with no thermal loading was 69.5 hours. Recall that the experimentally measured time was 7.3 hours. In [6] Gerdeen and Sazawal present a closed form solution for this particular problem and they cite a critical time of 21.6 hours. It is a generally accepted belief that experimental buckling results can differ greatly from analytical results due to initial imperfections, eccentricities, or differences in applied boundary conditions. The critical time estimate given by the finite element model could not be attributed to this behavior in light of the analytical results presented by Gerdeen and Sazawal. The finite element results were subsequently attributed to a stiff finite element mesh.

Major modifications in the cylinder model were made by changing from continuum type elements to axisymmetric isoparametric shell elements and by increasing the number of elements along the length to fifty (see Fig. 2b). The number of elements decreased from 60 to 50 but the number of degrees of freedom increased from 160 to 200. Calculation of the instantaneous elastic buckling load now produced a result within five percent of the classical value. The shell was again creep analyzed to a time of one hour and the time of collapse was estimated to be 19.7 hours, which correlates well with the analytical estimate of 21.6 hours.

A comparison of the displacement solutions from both models revealed, as expected, that the second model is the more flexible. The radial displacements are essentially the same for points located away from the shell edge that is radially restrained. Near this edge, however, the cylinder experiences large radial deformations which must be modeled accurately if the true behavior is to be predicted. The location of this radial bulge differed for the two meshes. The second model had the maximum radial displacement occurring 14 mm from the edge, in comparison to 20 mm for the first model. It is felt that the first model was too coarse locally to allow the radial bulge to develop naturally near the edge and, by forcing the bulge further away, an incorrect buckling mode shape was calculated; consequently, the critical time was incorrectly estimated.

If the creep analysis is extended up to a maximum of five hours, the estimate of critical time is increased to 20.9 hours. A plot of real (creep) time versus estimated collapse time shows that this data can be extrapolated to predict an upper bound of 21 hours (see Fig. 3). The change in the critical time over the five hour period was six percent.

An attempt was made to correlate with Samuelson's experimental result by incorporating the effect of the pre-test thermal expansioin into the numerical model. The thermal data for the material was taken from Bushnell [7]. The presence of the thermal expansion lowered the estimated critical time from 19.7 to 18.3 hours--still significantly above the experimentally determined value. The equivalent tensile stress calculated in this analysis, for the combined thermal and mechanical loading, was observed to be larger than the yield stress reported by Samuelson for this material. This fact led to some speculation that the actual collapse of the test specimen was due to the presence of plasticity in the region near the shell supports. The combined elastic/plastic-creep behavior was subsequently analyzed, resulting in a nonpositive definite stiffness at 9.56 hours. The instability was due to the formation of a plastic hinge near the restraining edge.

The direct method could not be used in this instance to calculate the critical buckling time because of the presence of large plastic strains. The critical time was determined by marching in time until the structural stiffness became nonpositive definite. Results obtained by this procedure agree very well with the experimentally determined value; the remaining differences can be attributed to further shell imperfections and to inaccuracies in modeling the creep behavior.

The structural instability predicted by the finite element analysis was the product of a complex interaction between creep deformation and plasticity. Initial application of the test load caused local yielding in elements near the shell supports with the plasticity occurring through a quarter of the wall thickness. The ensuing creep analysis caused the load to redistribute across the wall thereby lowering the maximum stresses to a value below the yield stress. As the creep analysis progressed these values remained below yield until the creep-induced deformations caused enough bending to once again bring the maximum stress above yield. This occurred at 6.8 hours of creep time. At this time the plastic zone begins to spread through the wall, more or less proportionately to the magnitude of the creep-enhanced deformation. At 9.56 hours the plastic region had spread through the wall and a plastic hinge developed, causing the structural instability.

Another question which was addressed during this study was the effect of primary creep on the estimated critical times. A creep law which includes both primary and secondary creep models was inserted into the numerical model. This creep law is given by

$$\dot{\bar{\varepsilon}}_c = A(1 - e^{-\alpha t}) + B\bar{\sigma}^n \quad . \tag{10}$$

The constant A was determined by creep data supplied by Samuelson and the parameter, α, was varied. It was found that critical time estimates taken during the primary creep stage were lower than those predicted during secondary creep. This is not a surprising result when one considers that the

creep rate is highest during primary creep so that a critical time estimate would reflect the large initial strain terms and predict an early collapse. As the model passed from the primary to the secondary stage, the estimated times assumed the values previously reported with no primary creep. In analyzing nuclear piping components the period of primary creep is a small portion of the service life and can be omitted from this type of analysis.

In this report, the main interest has been centered around problems characterized by continued application of the applied loads for long hold times. The question of how to treat load reversals and subsequent reintroduction of primary creep behavior has not been addressed.

The studies described in the preceding paragraphs were undertaken to qualify the nonlinear, finite element code for the prediction of time-dependent buckling behavior. The remainder of the discussion is directed toward the ultimate goal of determining the conservatism of current ASME design rules for time-dependent, load-controlled buckling. Previously, a factor of ten on service life was required, but this has recently been replaced with load factors of safety which are believed to be equivalent to the factor of ten on service life. These load factors are 1.5 for normal, upset, and emergency operating conditions, and 1.25 for faulted operating conditions.

The aluminum cylinder model was selected to represent a typical piping component being analyzed according to the design rules governing time-dependent buckling. Although the particular material identified in this study is aluminum, the results are felt to be relevant to a wide variety of nuclear structural materials operating at elevated temperature. The cylinder had both mechanical and thermal loads applied and the secondary creep model was of the power law type. Critical time estimates were obtained over a range of secondary creep exponents. The applied mechanical loads were then increased by fifty percent and a new set of critical times was calculated. The critical times, corresponding to the design load and 1.5 times the design load, are plotted in Fig. 4, as a function of creep exponent.

To interpret these results in light of the past and present design rules, consider a nuclear piping component with a hypothetical service life of 15 hours and a secondary creep exponent of 5. The current design rules are satisfied by the 16.23 hour critical time estimate taken from the 18.1 kg/mm^2 curve in Fig. 4, but the requirement of a factor of ten on service life (150 hours) is not satisfied by the 117 hour critical time estimate taken from the 12.1 kg/mm^2 curve. In this particular example, the two design rules are not equivalent and the current requirement regarding the load safety factor is not as conservative as the rule it replaces. It is possible, however, to select an example such that the design rules are equivalent for a creep exponent of 5. Suppose the required service life was ten hours; then the estimates of critical time taken from Fig. 4 satisfy both design requirements and the rules are said to be equivalent.

This confusing situation exists for those values of creep exponent

whose critical time estimates differ by less than a factor of ten. In this situation, the current load safety factor rule is conservative or nonconservative, depending upon the margin of safety in the buckling analysis. This was illustrated by the previous examples. For creep exponents with factors greater than ten, the design rules are always equivalent.. Fig. 5 is a plot of the time factors as a function of creep exponent. Note that the past and present design rules are equivalent at the higher creep exponents (>6).

V. Conclusions and Recommendations

The current study was conducted in an effort to determine the degree of conservatism or lack of conservatism in current ASME design rules concerning time-dependent (creep) buckling. In the course of this investigation, certain observations were made concerning the numerical solution of creep buckling problems. It was demonstrated that a nonlinear finite element code could be used to solve the time-dependent buckling problem. A direct method of solution was presented which proved to be computationally efficient and provided answers which agreed very well with available analytical solutions.

It was observed that the calculated buckling times could vary widely for small errors in computed displacements. Care must be taken when discretizing such problems to refine the mesh in areas where large time-dependent deformations are likely to occur. A suggested procedure for determining a suitable grid would be to mesh the problem using a coarse grid. Solve the static and time-dependent problems and inspect the solution for the presence of large deformation gradients. In those areas where large gradients are present, refine the mesh, and solve for the critical buckling time. This procedure should ensure a reasonable solution for a minimum of computational effort.

Data for the creep model was taken from experimental work by Samuelson and a power law representation was assumed based on his results. The model was modified for evaluation of primary creep effects on the calculation of critical time estimates. The presence of high creep strain rates contributed to the prediction of early buckling times when calculated during the primary creep stage. The predicted time estimates were found to increase with time until the secondary stage was reached and the estimates approached the critical times predicted without primary creep. It can be concluded, therefore, that for most nuclear piping components, whose primary creep stage is small compared to the secondary stage, the effect of primary creep is negligible and can be omitted from the calculations.

In an evaluation of the past and current ASME design rules for time-dependent, load controlled buckling, it was concluded that current use of design load safety factors is not equivalent to a safety factor of ten on service life for low creep exponents. Calculations were presented which showed that the current rules were nonconservative, compared to the previous

rules, for creep exponents below the value of six. Creep exponents above that value were shown to give equivalent results for both rules. It is expected that the exact cutoff between conservative and nonconservative exponents will vary according to the problem but the same nonconservative results will be observed at the lower exponents.

Future work in this area will be addressing the problem of time-dependent buckling for an actual LMFBR piping component. A standard long radius pipe elbow has been chosen as the particular geometry. A three-dimensional finite element analysis of this is planned, employing the same methods described in this report, and the results are to be compared with experimental data from either United States or foreign sources.

References

[1] I. Berman, A. C. Gangadharan, and G. D. Gupta, "Buckling and Instability at Elevated Temperatures," Advances in Design for Elevated Temperature Environment, S. Y. Zamrik and R. I. Jetter, eds., American Society of Mechanical Engineers (June 1975).

[2] L. A. Samuelson, "Experimental Investigation of Creep Buckling of Circular Cylindrical Shells Under Axial Compression and Bending," J. Engr. and Ind., 90, 589-595 (1968).

[3] N. Miyazaki, G. Yagawa, and Y. Ando, "A Parametric Analysis of Creep Buckling of Shallow Spherical Shell by the Finite Element Method," American Society of Mechanical Engineers Preprint No. 76-PVP-45, June 1976.

[4] H. D. Hibbitt, P. V. Marcal, and J. R. Rice, "A Finite Element Formulation for Problems of Large Strain and Large Displacement," Intl. J. of Solids and Structures, 6, 1069-1086 (1970).

[5] G. A. Dupuis, D. D. Pfaffinger, and P. V. Marcal, "Effective Use of the Incremental Stiffness Matrices in Nonlinear Geometric Analysis," Proceedings IUTAM Symposium on High Speed Computing of Elastic Structures, Liege, Belgium (1970).

[6] J. C. Gerdeen, and V. K. Sazawal, Review and Interpretive Report on Creep Instability, Vol. I, Department of Mechanical Engineering and Engineering Mechanics, Michigan Technological University, Houghton, MI (1973).

[7] D. Bushnell, "BOSOR5-Program for Buckling of Elastic-Plastic Complex Shells of Revolution Including Large Deflections and Creep," Computers and Structures, 6, 221-239 (1976).

List of Figures

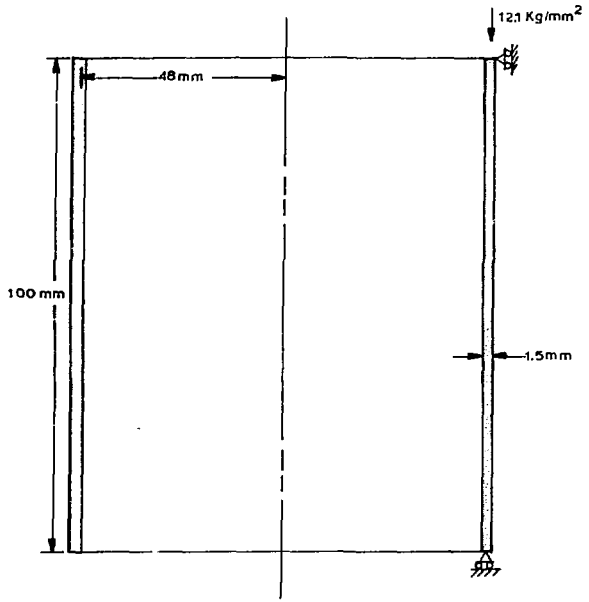

$E = 5830$ Kg/mm^2 CREEP LAW: $\dot{\bar{\epsilon}}_c = A\sigma^n$

$\nu = .3$ $n = 5.8$

$A = 4.4 \times 10^{-10}$ Hr^{-1}

AXISYMMETRIC RING ELEMENTS

20 ELEMENTS AXIALLY
3 ELEMENTS RADIAL

FIGURE 2A

AXISYMMETRIC ISOPARAMETRIC SHELL ELEMENTS

50 ELEMENTS

FIGURE 2B

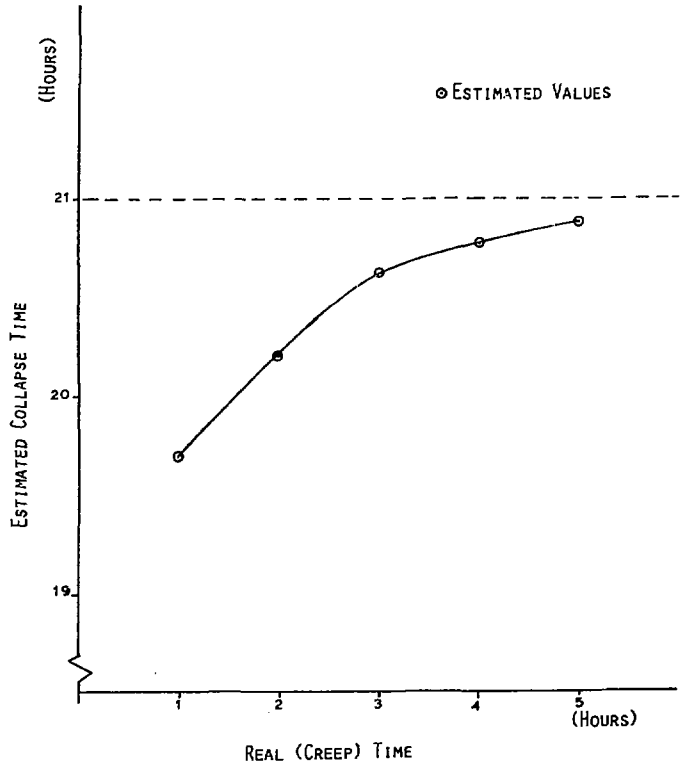
(HOURS)
⊙ ESTIMATED VALUES
21
20
19
ESTIMATED COLLAPSE TIME
1
2
3
4
5
(HOURS)
REAL (CREEP) TIME

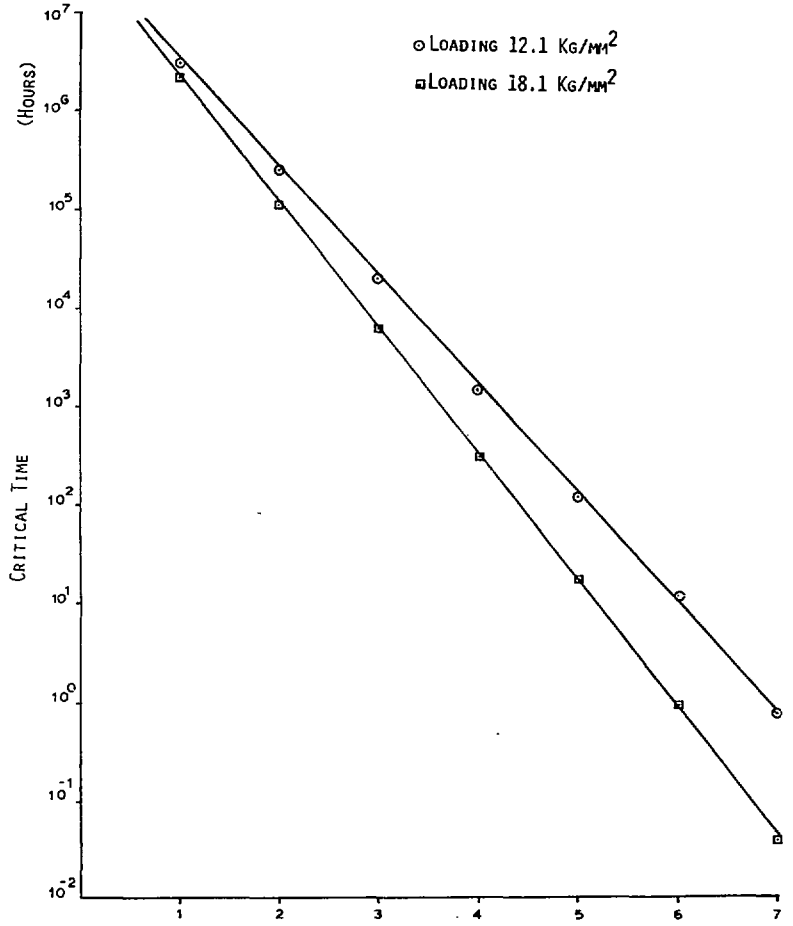
⊙ LOADING 12.1 KG/MM2
⊡ LOADING 18.1 KG/MM2
CRITICAL TIME (HOURS)
10^7
10^6
10^5
10^4
10^3
10^2
10^1
10^0
10^-1
10^-2
1
2
3
4
5
6
7

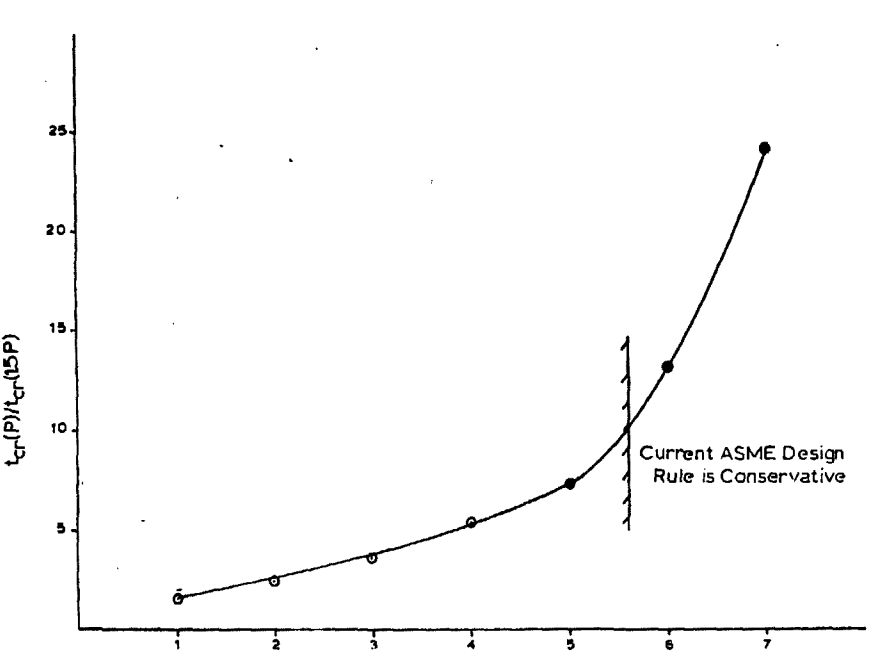
$t_{cr}(P)/t_{cr}(15P)$
25
20
15
10
5
1
2
3
4
5
6
7
Current ASME Design
Rule is Conservative